

077  
G-80-077

# Viking Orbiter 75 In-Flight Pointing Calibration of the High-Gain Antenna

Touraj Assefi\* and James W. Alexander†

*Jet Propulsion Laboratory, California Institute of Technology, Pasadena, Calif.*

An in-flight pointing calibration technique developed for the Viking Orbiter high-gain antenna has been validated through actual flight usage. The desired telecommunications performance dictated that the high-gain antenna pointing error be held at 0.7 deg, which would have been exceeded without calibration. The in-flight calibration methodology required the development of a stochastic model of the spacecraft rotational biases and Earth-received signal strength measurements. The signal strength measurements, which were performed at X-band frequency, were used as observations to estimate the rotational biases and their corresponding uncertainties. Reducing the uncertainties of these parameters resulted in increased antenna pointing accuracy. The initial pointing offset was estimated to be in excess of 1 deg, and after in-flight calibration it was reduced to about 0.66 deg. About 50% of the original offset could not be calibrated, thus the improvement on the remaining offset is better than 50%.

## Nomenclature

$a$	= parameter dependent on antenna dish characteristics
$A, B, C$	= axes of celestial fixed coordinate system
AGC	= ground measurement of antenna signal strength in dB
DN	= telemetry data number
$\tilde{e}_A$	= error vector mapped to HGA coordinate system
$e_i$	= error parameters to be estimated
HGA	= high-gain antenna
IFCAL	= computer program used to determine error parameters
$Q_0$	= coordinate system determined by $A, B, C$
$Q$	= coordinate system determined by $X, Y, Z$
$Q_i$	= coordinate system determined by $X_i, Y_i, Z_i$
$Q', Q_0'$	= coordinate system obtained from $Q, Q_0$ by correcting for spacecraft oscillations
$S$	= signal strength measurement
$S_0$	= signal strength parameter dependent on spacecraft range
$T'_{II}$	= transformation from coordinate systems I to II
$\hat{V}_e$	= unit spacecraft Earth vector
VO	= Viking Orbiter
VO1	= Viking Orbiter 1
VO2	= Viking Orbiter 2
$v(t)$	= noise measurement
X-band	= HGA carrier frequency used for calibrations
$X, Y, Z,$ $X_i, Y_i, Z_i$	= $x, y, z$ axes in various coordinate systems
$x(t)$	= state to be estimated
$\hat{x}(t)$	= estimate of $X(t)$
$y(t)$	= measurement of noisy signal strength
$\alpha_X$	= clock angle of spacecraft $X$ axis
$\beta_s$	= cone angle of reference star
$\delta S, \delta S_0$	= changes in $S, S_0$
$\rho$	= HGA boresight Earth offset

## Introduction

THIS paper describes an in-flight calibration methodology for the Viking Orbiter high-gain antenna (HGA). The HGA in-flight calibration was first demonstrated for the Mariner Venus-Mercury 1973 (MVM-73).<sup>1,2</sup> The Viking calibration procedure is partially based on techniques developed in MVM-73. The Viking Orbiter telecommunication performance required the HGA pointing error to be held to less than 0.7 deg ( $3\sigma$ ). This pointing error is defined as the total HGA pointing error of the HGA electrical boresight with respect to the spacecraft Earth vector. The initial antenna pointing offset was in excess of 1 deg. This offset is a function of errors that can be divided into two types—control-type errors and knowledge-type errors. The former consists of those errors for which the ground calibration is sufficient or not possible and cannot be calibrated in-flight. The latter consists of those errors for which the ground calibration is insufficient and can be calibrated in-flight. Two of the dominant error sources, the limit cycle motion (0.25 deg/axis) and the antenna pointing resolution (0.16 deg) are the control type errors. These errors typically contribute a value up to 0.5 deg. The effect of in-flight calibration is to replace all knowledge-type fixed offsets with a “pointing knowledge error” or “residual in-flight calibrating error” which, together with the control-type errors, determine the total pointing offset.

In general, one can assume that the HGA pointing error is a function of rotational error sources that tend to change in the course of time. In order to estimate the rotational offsets and reduce their associated uncertainties, which in turn reduces the uncertainty of HGA pointing, an extensive error model of these offsets and their uncertainties was developed. In-flight calibration is the process of estimating corrections to knowledge-type error parameters and, since these error parameters are stochastic, a stochastic model for the in-flight calibration was developed. The model used signal strength measurements conducted at X-band frequencies as inputs. Any deviation from peak signal strength was assumed to be entirely due to the spacecraft-related pointing errors. Any X-band variation that did not contribute to the pointing error was considered to be a source of noise in the measurements. Using the stochastic model and taking several successive in-flight measurements before Mars encounter yielded more accurate offset values and associated uncertainties. These calibrations showed that the pointing requirement had been achieved. The estimated error reduction from the un-

Received April 5, 1979; revision received Oct. 29, 1979. Copyright © American Institute of Aeronautics and Astronautics, Inc., 1979. All rights reserved.

Index categories: Guidance and Control; Data Sensing, Presentation, and Transmission.

\*Group Leader, Guidance and Control Section.

†Engineer, Automated Systems Section.

calibrated value of more than 1 deg to about 0.66 deg was accomplished even though the control-type errors contributed to more than 50% of the total HGA pointing error. The in-flight calibration technique developed in this paper can be applied to other spacecraft where signal strength measurements are used as inputs to the estimation algorithm.

### Mathematical Error Modeling

The Viking HGA is mounted on a two-degree-of-freedom azimuth and elevation gimbaled support structure, where its movement is controlled by two mutually orthogonal stepper motor actuators. Figure 1 shows the HGA relative to the rest of the Viking spacecraft, and indicates the Orbiter XYZ body-fixed coordinate system. All other spacecraft coordinate systems are related to this XYZ system.

#### Coordinate Systems

The celestial coordinate system denoted by  $Q_0$  is used as a reference coordinate system and is completely determined by the sun and a reference star. The definition of  $Q_0$  as well as the other coordinate systems are given below.

$Q_0$  is the celestially fixed ( $A, B, C$ ) axis coordinate system, where  $C$  is the probe-sun unit vector, and

$$B = (C \times S) / |C \times S|$$

where  $S$  is the probe-reference star unit vector;  $A = B \times C$  completes the orthogonal system.

$Q$  is the spacecraft body axis (pitch, yaw, roll) coordinate system ( $X, Y, Z$ ) and is shown in Figs. 1 and 2. The relationship between  $Q_0$  and  $Q$  is also shown.

$Q_1$  = azimuth actuator coordinate systems ( $X_1, Y_1, Z_1$ )

$X_1$  = azimuth hinge axis being in the  $XY$  plane

$Y_1 = (Z \times X_1) / |Z \times X_1|$

$Z_1 = Z$

$Q_2$  = elevation actuator hinge coordinate system

$X_2 = X_1$

$Y_2$  = elevation actuator axis

$Z_2 = X_2 \times Y_2$

$Q_3$  = the antenna coordinate system

$X_3 = Y_3 \times Z_3$

$Y_3 = Y_2$

$Z_3$  = antenna boresight (see Fig. 3 for  $Q_1, Q_2$ , and  $Q_3$ )

$Q'$  is the spacecraft actual coordinate system, obtained from  $Q$  by a sequence of rotations around the pitch, yaw, and roll axis, respectively. That is,  $Q'$  is obtained from  $Q$  by  $\text{Rot}(r) \text{Rot}(y) \text{Rot}(p)$ , where  $\text{Rot}(\cdot)$  denotes the orthogonal transformation around the indicated axis.

$Q'_0$  is the spacecraft fixed coordinate system ( $A', B', C'$ ).

#### Identification of Biases Affecting the Pointing Accuracy of the HGA

The following notation will be used in the subsequent work to define the rotational error vectors:

$\bar{e}_1 \triangleq$  error vector in the spacecraft body axis coordinate system ( $X, Y, Z$ )

$\bar{e}_2 \triangleq$  error vector in the azimuth actuator coordinate system ( $X_1, Y_1, Z_1$ )

$\bar{e}_3 \triangleq$  error vector in the elevation actuator coordinate system ( $X_2, Y_2, Z_2$ )

$\bar{e}_4 \triangleq$  error vector in the antenna coordinate system ( $X_3, Y_3, Z_3$ )

Using these coordinate transformations, each rotational error vector  $\bar{e}_i$  can be mapped to the same antenna coordinate system. The resultant error vector in the antenna coordinate system is denoted as  $\bar{e}_A$ .

It can be shown that the first-order antenna rotational error  $\bar{e}_A$  can be written as

$$\begin{aligned} \bar{e}_A &= \bar{e}_4 + T_{Q_3}^{Q_2} \bar{e}_3 + T_{Q_3}^{Q_2} T_{Q_2}^{Q_1} \bar{e}_2 + T_{Q_3}^{Q_2} T_{Q_2}^{Q_1} T_{Q_1}^{Q_0} \bar{e}_1 \\ &= \bar{e}_4 + T_{Q_3}^{Q_2} \bar{e}_3 + T_{Q_3}^{Q_1} \bar{e}_2 + T_{Q_3}^{Q_0} \bar{e}_1 \end{aligned} \quad (1)$$

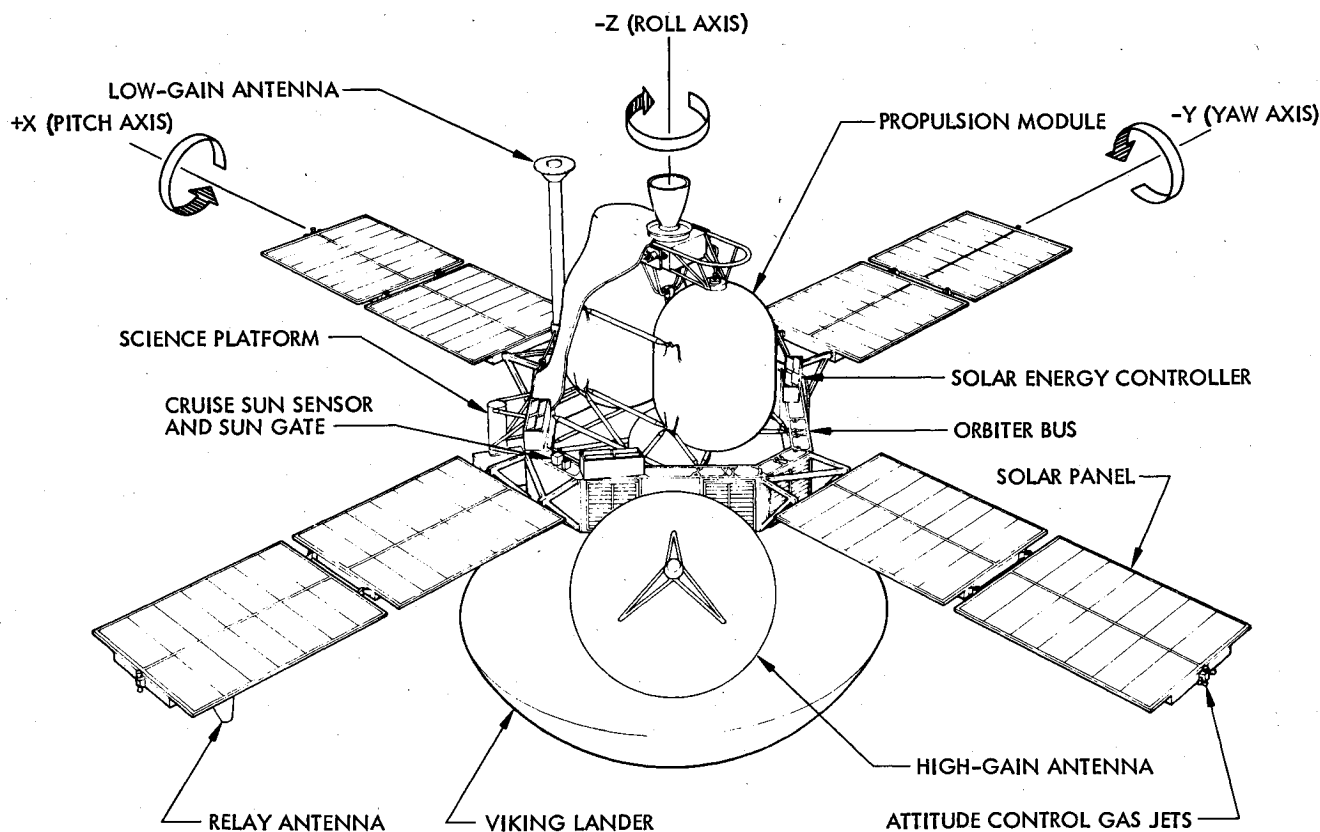


Fig. 1 Viking Orbiter configuration and coordinate system.



Then  $Z(t)$  can be rewritten as

$$Z(t) = C(t)W(t) + v(t) \quad (8)$$

and  $C(t)$  is given by

$$C(t) = \left( \frac{\partial \delta S}{\partial x} \right)_{x=x_0} = \left( \frac{\partial Z}{\partial x} \right)_{x=x_0} \quad (9)$$

where  $\delta S$  is the perturbed signal of  $S$  given by

$$\delta S = \delta S_0 + \log_{10} [(\sin \alpha \rho) / \alpha \rho]^2 \quad (10)$$

Therefore,  $C(t)$  is a row vector of order 12 and it can be partitioned as follows:

$$C = [C_1 \mid C_2] = [c_1 c_2 \dots c_{10} \mid c_{11} c_{12}]$$

where  $C_1$  and  $C_2$  are given by

$$C_1 = \frac{\partial \delta S}{\partial (x_1, \dots, x_{10})} = \frac{\partial \delta S}{\partial \bar{e}_A} \frac{\partial \bar{e}_A}{\partial (x_1, \dots, x_{10})} \quad (11)$$

and  $C_2$  by

$$C_2 = \left[ I, \frac{20}{\log_e 10} \frac{(\alpha \rho) \cos \alpha \rho - \sin \alpha \rho}{\alpha \sin \alpha \rho} \right] \quad (12)$$

where

$$\frac{\partial \delta S}{\partial \bar{e}_A} = \frac{10}{\log_e 10} f(\rho) \cos(0, 0, 1) \frac{\partial}{\partial \bar{e}_A} (\hat{V}_E)$$

$\hat{V}_E$  = Orbiter-Earth unit vector

$$f(\rho) \triangleq 2 \frac{\sin \alpha \rho - \alpha \rho \cos \alpha \rho}{\rho \sin \alpha \rho \sin}$$

and

$$\begin{aligned} \frac{\partial \bar{e}_A}{\partial x_1} &= \cos[0, 0, 1] & \frac{\partial \bar{e}_A}{\partial x_2} &= \cos[0, 1, 0] \\ \frac{\partial \bar{e}_A}{\partial x_3} &= \cos[1, 0, 0] & \frac{\partial \bar{e}_A}{\partial x_4} &= T_{Q_3}^{Q_2} \cos[0, 0, 1] \\ \frac{\partial \bar{e}_A}{\partial x_5} &= T_{Q_3}^{Q_1} \cos[0, 1, 0] & \frac{\partial \bar{e}_A}{\partial x_6} &= T_{Q_3}^{Q_1} \cos[1, 0, 0] \\ \frac{\partial \bar{e}_A}{\partial x_7} &= T_{Q_3}^{Q_1} \cos[0, 0, \cot \beta_s] & \frac{\partial \bar{e}_A}{\partial x_8} &= T_{Q_3}^{Q_1} \cos[0, 0, 1] \\ \frac{\partial \bar{e}_A}{\partial x_9} &= T_{Q_3}^{Q_1} \cot[0, 1, \sin \alpha_x \cot \beta_s] \\ \frac{\partial \bar{e}_A}{\partial x_{10}} &= T_{Q_3}^{Q_1} \cos[1, 0, \cot \beta_s \cos \alpha_x] \end{aligned}$$

The noise  $v(t)$  is given by

$$v(t) = \sum_{i=1}^6 b_i v_i(t)$$

where  $b_1 = c_2, b_2 = c_6, b_3 = c_8, b_4 = c_9, b_5 = c_{10}, b_6 = c_{11}$ . The  $b_i$ 's are constant during each calibration,  $v_1, v_2, \dots, v_5$  are telemetry noise sources, and  $v_6$  is the signal strength noise source.

The best mean-square estimate of  $x$  denoted by  $\hat{x}$  and its associated covariance matrix at the  $(k+1)$  in-flight calibration resulting from a set of  $I$  signal-strength

measurements can be obtained in the usual way [Eq. (1)]. However, for the sake of completeness they are listed as follows:

$$\hat{x}_{k+1} = P_{k+1} \left[ \sum_{i=1}^I C' \sigma^{-2} y_{k+1}(i) + P_k^{-1} \hat{x}_k \right] \quad (13)$$

$$P_{k+1} = \left[ P_k^{-1} + \sum_{i=1}^I C' \sigma^{-2} C \right]^{-1} \quad (14)$$

where  $I$  is the number of observations (AGC measurements) in each calibration,  $\hat{x}_0$  is the a priori estimate of  $x$ ,  $P_0$  is a covariance matrix corresponding to  $\hat{x}_0$ , and  $\sigma$  is the standard deviation of observation noise.

### Implementation and Results

The following describes: 1) the general data gathering and calibration procedures used to perform an X-band calibration, 2) the analysis and results from a single VO1 calibration, and 3) the general results from the VO2 calibrations. Table 1 shows the dates of each valid calibration, and the position of the Earth in azimuth-elevation coordinates at that time. No use could be made from the data obtained by calibrations 3 and 6 for VO1 and 3 for VO2.

### Calibration Procedure and Data Gathering

A typical HGA calibration was performed by moving the HGA in a box-like pattern about the nominal position of the Earth. A typical pattern is shown in Fig. 5, where the nodes indicate positions where the HGA stopped for approximately 8 min and data were taken. Ten to twelve nodes were required per calibration, so about 90 min were needed to complete the sequence. In addition, the time of day of the calibration had to be chosen so that the Orbiter would remain high enough above the horizon of the Earth during the calibration procedure to allow consistent tracking station signal strength measurements.

In order to compute the position of the Earth relative to the Orbiter and the Orbiter celestially based coordinate system, Orbiter geometry information was computed from Orbiter trajectory data (which had been determined from radio tracking results). Telemetry measurements from the Orbiter (transmitted at a rate of 33 bits/s) provided data numbers (DN) for: 1) fine and coarse feedback potentiometers for the azimuth and elevation HGA actuators (one reading every 430.08 s) and 2) relative position readings for the celestial sensors (one reading every 6.72 s). This data was converted to engineering units (deg, etc.), and was used to compute the nominal position of the HGA relative to the celestial coordinate system. The HGA X-band signal strength measurements were provided by a 64-m tracking station, which was used to compute the signal strength loss. This data in turn was used to compute the angular displacement of the HGA boresight from the Earth. These sets of data were then merged to provide the appropriate set of input for the calibration analysis programs.

Table 1 Dates of valid calibration

VO/cal. no.	Earth		Day-1976
	azimuth, elevation, deg		
VO1/1	7.2,	29.5	6 (Jan 6)
VO2/1	5.4,	31.9	9 (Jan 9)
VO1/2	5.2,	37.3	33 (Feb 2)
VO2/2	5.1,	38.4.	38 (Feb 7)
VO1/4	5.7,	39.4	70 (Mar 10)
VO2/4	6.7,	39.5	78 (Mar 18)
VO1/5	6.2,	38.7	87 (Mar 27)
VO2/5	7.6,	35.8	120 (Apr 29)

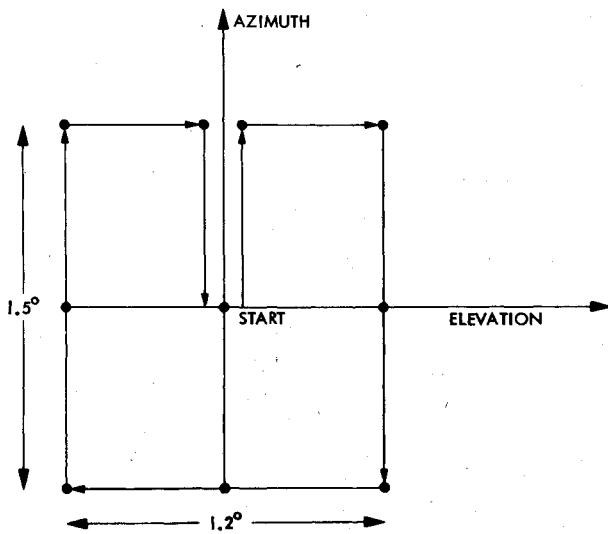


Fig. 5 HGA calibration pattern.

In order to compute the position of the Earth relative to the Orbiter and the Orbiter celestial based coordinate system, Orbiter geometry information was computed from Orbiter trajectory data (which had been determined from radio tracking results). Telemetry measurements from the Orbiter (transmitted at a rate of 33 bits) provided data numbers (DN) for: 1) fine and coarse feedback potentiometers for the azimuth and elevation HGA actuators (one reading every 430.08 s) and 2) relative position readings for the celestial sensors (one reading every 6.72 s). This data was converted to engineering units (deg, etc.), and was used to compute the nominal position of the HGA relative to the celestial coordinate system. The HGA X-band signal strength measurements were provided by a 64-m tracking station, which was used to compute the signal strength loss. This data in turn was used to compute the angular displacement of the

HGA boresight from the Earth. These sets of data were then merged to provide the appropriate set of input for the calibration analysis programs.

#### Calibration Analysis

The following describes the results of the calibration analysis performed on data from the fifth VO1 calibration (executed on day 86, 1976). The results (correction estimates, covariance matrix) from the fourth VO1 calibration were used as the initial data for this analysis. Given this initial estimate and the merged data described earlier, the bulk of the remaining analysis was done by the IFCAL program.

The slewing pattern for this calibration was the usual box, allowing an excursion of  $\pm 0.75$  deg in the elevation and  $\pm 0.6$  deg in azimuth (see Fig. 5) from the nominal position of the Earth—6.27 deg azimuth and 38.81 deg elevation. Limit cycle contributions were limited to 0.25 deg offset per axis, allowing for a maximum HGA boresight-Earth offset of 1.2 deg.

Figure 6 shows the raw signal strength loss (in dB) as a function of HGA position before any noise filtering or other processing was done. The dots represent AGC measurements, which were taken about 30 s apart. The HGA position numbers (horizontal axis) refer to Fig. 5, position 1 being the starting point, etc. During this particular calibration, the limit cycle position of the Orbiter varied slowly (the nominal half-period is 20 min), so there is only a small AGC drift apparent at each HGA position. Data obtained near the time of a slew has been removed to eliminate possible timing errors and the effects of HGA settling that would affect the computed HGA pointing direction. During this calibration, there was a 3.3 dB loss of AGC from maximum signal strength. Using the X-band signal strength model given by Eq. (10), this indicates that the maximum boresight-Earth offset was about 0.9 deg. This allowed data to be obtained from the region of steeper signal strength slope without losing antenna lock.

Using the filter method described earlier, IFCAL iterated on a set of error correction terms so that the residuals (the difference between the measured signal strength and the

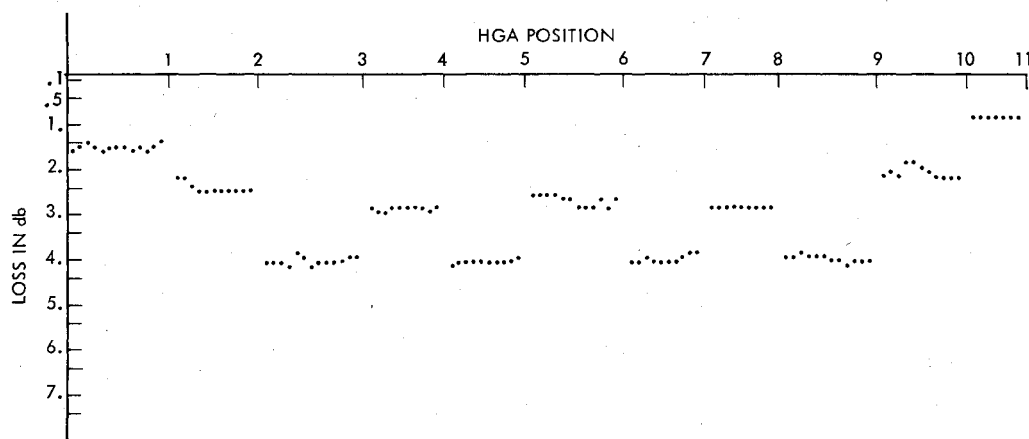


Fig. 6 AGC loss from maximum vs HGA position.

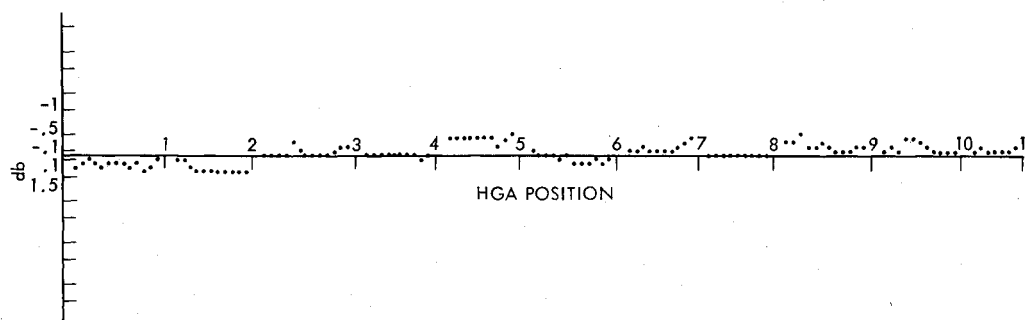


Fig. 7 Residuals (dB) vs HGA position.

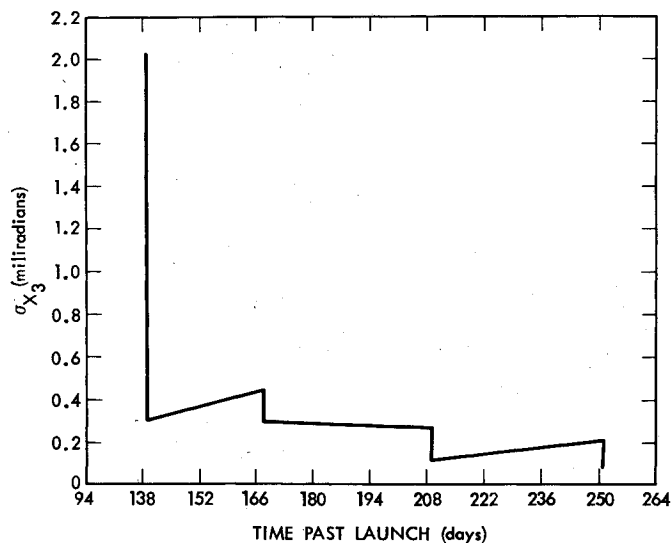


Fig. 8 VO2 X-axis uncertainties vs time.

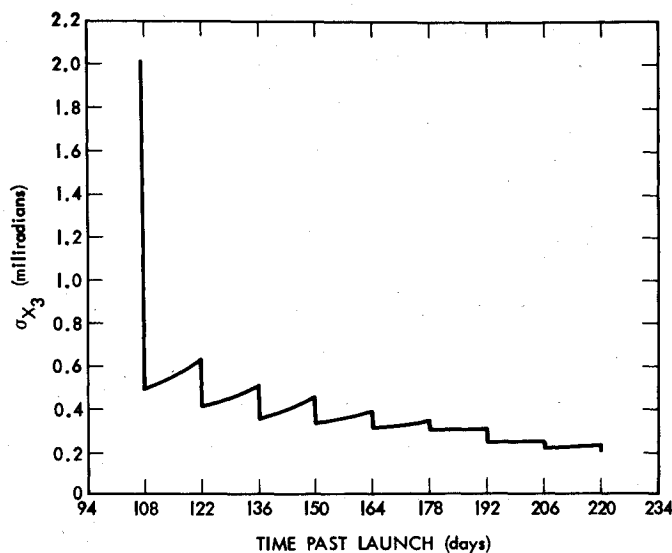


Fig. 10 Simulation results for X axis.

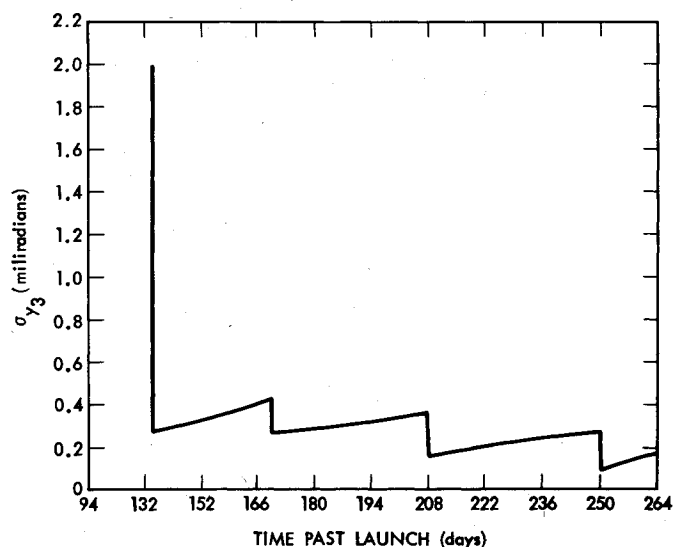


Fig. 9 VO-2 Y-axis uncertainties vs time.

signal strength predicted from these correction terms and the HGA X-band model) were minimized in the mean square sense. Figure 7 shows the residuals from this calibration as a function of the HGA position. For this calibration, the mean of these residuals was 0.03 dB, with a standard derivation of 0.26 dB. Included in this error uncertainty figure is some tracking station drift and a 0.1 dB uncertainty in the AGC data measurements.

#### General Results

In general, the results of using the correction factors calculated in the manner described have been excellent. Daily radio science measurements have shown little deviation from the expected signal strength (although radio science primarily used S-band, which has a wider pattern than the X-band that was used for these calibrations). More precise corroboration has been obtained from examining the uncertainties and error parameters associated with the set of HGA calibrations as a whole. After a typical calibration, the resulting error parameters show a signal strength error of 0.25 dB (less than

0.1 deg). After the first HGA calibration the error parameters changed only a little, indicating that a correct set had been obtained. Figure 8 shows the uncertainty associated with the X (pitch) axis as a function of time past launch date and Fig. 9 the uncertainty of the Y (yaw) axis determined from the actual calibration data. Figure 10 shows the results of a prelaunch simulation for the X axis. Comparing Fig. 8 and Fig. 10, it is clear that the actual results agree closely with the simulation. Using the estimated error of 0.5 deg from other uncalibratable sources, a 0.1 deg error uncertainty in performance of a calibration, a  $3\sigma$  uncertainty of 0.06 deg due to not updating parameters between calibrations, show a total pointing error to be less than  $0.5 + 0.1 + 0.06 = 0.66$ , less than the required 0.7 deg.

#### Conclusions

The feasibility of the HGA in-flight calibration technique has been demonstrated for the X-band radio frequency communication system. The in-flight calibration of the HGA has significantly improved its pointing accuracy, and the uncertainties of all the biases have been considerably decreased. Figures 8-10 show the improvements of the standard deviations of the X and the Y axes as a function of time past launch (days). Without the in-flight calibration, the pointing requirement of the HGA boresight would have not been met.

#### Acknowledgments

This paper presents the results of one phase of research carried out at Jet Propulsion Laboratory, California Institute of Technology, under Contract NAS 7-100.

#### References

- Hardman, J.M., Havens, W.F., and Ohtakay, H., "In-Flight Calibration of the High Gain Antenna Pointing for the Mariner Venus-Mercury 1973 Spacecraft," Jet Propulsion Lab., Technical Memo. 33-740, Oct. 15, 1975.
- Ohtakay, M. and Hardman, J.M., "In-flight Calibration Technique for Onboard High-Gain Antenna Pointing," *Journal of Spacecraft and Rockets*, Vol. 12, Dec. 1975, pp. 754-759.
- Assefi, T., *Stochastic Processes and Estimation Theory with Applications*, John Wiley, New York, 1979.
- Sage, A.P. and Melsa, J.T., *Estimation Theory with Applications to Communications and Control*, McGraw-Hill, New York, 1971.